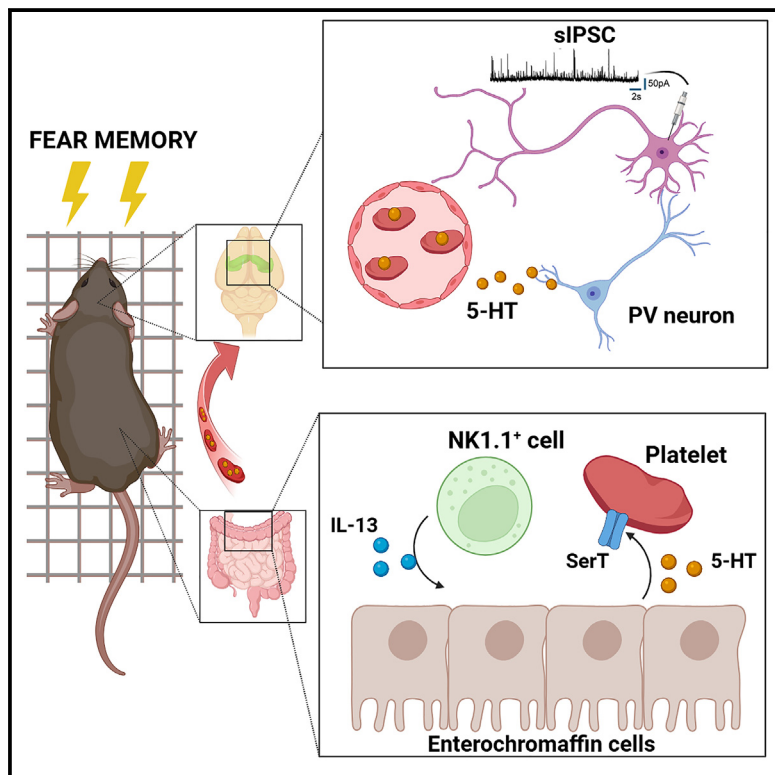


Platelets tune fear memory in mice

Graphical abstract



Authors

Stefano Garofalo, Alessandro Mormino, Letizia Mazzarella, ..., Myriam Catalano, Lucia Stefanini, Cristina Limatola

Correspondence

stefano.garofalo@uniroma1.it (S.G.), cristina.limatola@uniroma1.it (C.L.)

In brief

Garofalo et al. identify serotonin as a platelet-derived factor that modulates fear behaviors in mice through the control of inhibitory neurotransmission and plasticity in the hippocampus. Further, these findings highlight natural killer cells as central actors in contributing to the gut-platelet-brain dialogue.

Highlights

- Platelets are key link in body-brain communication in homeostasis
- Platelets tune parvalbumin neuron activity and long-term potentiation in the hippocampus
- Natural killer cells release IL-13 in the gut with effects on serotonin uptake by platelets
- Platelets and NK cells tune fear memory in mice



Article

Platelets tune fear memory in mice

Stefano Garofalo,^{1,8,*} Alessandro Mormino,¹ Letizia Mazzarella,¹ Germana Cocozza,¹ Arianna Rinaldi,¹ Erika Di Pietro,¹ Maria Amalia Di Castro,¹ Eleonora De Felice,¹ Laura Maggi,¹ Giuseppina Chece,¹ Diego Andolina,² Rossella Ventura,² Donald Ielpo,² Roberto Piacentini,^{3,4} Myriam Catalano,¹ Lucia Stefanini,⁵ and Cristina Limatola^{6,7,*}

¹Department of Physiology and Pharmacology, Sapienza University of Rome, Rome, Italy

²Department of Psychology and Center for Research in Neurobiology 'D. Bovet', Sapienza University of Rome, Rome, Italy

³Department of Neuroscience, Università Cattolica del Sacro Cuore, Rome, Italy

⁴IRCCS Fondazione Policlinico Universitario A. Gemelli, Largo A. Gemelli 1, Roma, Italy

⁵Department of Translational and Precision Medicine, Sapienza University of Rome, Rome, Italy

⁶Laboratory affiliated with Istituto Pasteur, Department of Physiology and Pharmacology, Sapienza University, Rome, Italy

⁷IRCCS Neuromed, Pozzilli, Italy

⁸Lead contact

*Correspondence: stefano.garofalo@uniroma1.it (S.G.), cristina.limatola@uniroma1.it (C.L.)

<https://doi.org/10.1016/j.celrep.2025.115261>

SUMMARY

Several lines of evidence have shown that platelet-derived factors are key molecules in brain-body communication in pathological conditions. Here, we identify platelets as key actors in the modulation of fear behaviors in mice through the control of inhibitory neurotransmission and plasticity in the hippocampus. Interfering with platelet number or activation reduces hippocampal serotonin (5-HT) and modulates fear learning and memory in mice, and this effect is reversed by serotonin replacement by serotonin precursor (5-HTP)/benserazide. In addition, we unravel that natural killer (NK) cells participate in this mechanism, regulating interleukin-13 (IL-13) levels in the gut, with effects on serotonin production by enterochromaffin cells and uptake by platelets. Both NK cells and platelet depletion reduce the activation of hippocampal inhibitory neurons and increase the long-term potentiation of synaptic transmission. Understanding the role of platelets in the modulation of neuro-immune interactions offers additional tools for the definition of the molecular and cellular elements involved in the growing field of brain-body communication.

INTRODUCTION

Bidirectional communication among the nervous and immune systems influences many physiological and pathological conditions. Peripheral neurons innervate lymphoid organs and provide additional modulatory mechanisms in innate and adaptive immunity.¹ On the other hand, different immune cell populations reside within the CNS,² where they are involved in regulating physiological functions and may contribute to or resolve pathological conditions.² Mice with severe combined immunodeficiency present cognitive impairment,³ and acute depletion of adaptive immunity impacts cognition, learning behavior, and hippocampal neurogenesis.^{4,5} In this scenario, little information is available about the role of platelets in modulating neuroimmune interactions.⁶ Platelets are anucleate cell fragments derived from megakaryocytes residing in the bone marrow and play key roles in hemostasis and thrombosis. Recent evidence has shown that platelets also have inflammatory and immune functions, releasing cytokines and attracting leukocytes to a site of injury.^{7–9}

Platelets are endowed with a number of intracellular granules, and their activation leads to the release of microvesicles (platelet-derived microvesicles [PMVs]) with a protein content highly dependent on the stimulus.¹⁰ Of interest, platelet delta granules store most of the peripheral serotonin, which repre-

sents 95% of the total body serotonin pool. Platelets do not synthesize serotonin, but, rather, take up circulating serotonin through a specific transporter (serotonin transporter [SERT]), mainly in the digestive tract and other regions.^{11,12} Platelet serotonin has been implicated in the regulation of gut-brain axis communication,¹³ and platelets and the content of their granules modulate neural precursors in brain neurogenic niches, such as the subventricular zone and the dentate gyrus.^{6,14,15} Platelet activation has been associated with neurodegenerative diseases¹⁶ such as Alzheimer's disease, and correlated evidence suggests some involvement in autism spectrum disorder.¹⁷ Interestingly, recent studies have identified CXCL4 and CXCR3 as potential mediators of platelet rescue effects in age-dependent cognitive decline.^{18,19}

Despite this increased knowledge of the involvement of platelet-derived signaling in neuropathologies, a neuromodulatory role of platelets in the healthy brain has never been described. Here, we investigated the hypothesis that platelets could mediate the neuroimmune interactions in the healthy brain, affecting synaptic transmission and behavior. We demonstrated that platelet depletion or inhibition by clopidogrel in mice reduces hippocampal serotonin levels and increases their performance in associative learning and memory fear behavioral tasks. This effect parallels reduced activation of parvalbumin neurons



and an increase in long-term potentiation (LTP) in the hippocampus. Notably, these effects of platelet depletion are also induced upon natural killer (NK) cell depletion, and NK cell-depleted mice have reduced levels of the SERT on the platelet surface and reduced interleukin-13 (IL-13) levels in the colon, the gut region where platelets take up serotonin.

Altogether, our data demonstrate that platelets are involved in regulation of neuroimmune interactions and able to modulate fear learning and memory under physiological conditions in mice.

RESULTS

NK cells modulate hippocampal serotonin levels and fear conditioning in mice

We have described recently that different subpopulations of NK cells and innate lymphoid cell 1 (ILC1) reside in the meningeal spaces and actively participate in anxiety-like behavior and non-spatial memory formation in mice.²⁰ Here, we investigated the potential role of NK cells in modulating additional behavioral domains, specifically learning and fear memory. We treated mice with an anti-NK1.1 antibody (Ab) (aNK1.1) to deplete the NK and NKT cell populations (which express the NK1.1 and NKp46 cell markers).^{20,21} The efficiency of NK cell depletion has already been shown^{20,22} and confirmed for this set of experiments. We have demonstrated previously that this treatment does not affect T cell differentiation, peripheral frequency, or homeostatic properties in lymphoid organs.²⁰ We studied the effect of NK cell depletion on consolidation of fear memory, taking advantage of a Pavlovian fear conditioning test, a behavioral paradigm that explores learning and reaction to aversive environmental stimuli. The data in Figure 1A show that NK cell-depleted mice have increased fear acquisition (day 1) and contextual fear responses (day 2), while no differences are observed in the cued fear responses (day 2) or in extinction of the fear memory 5 days after the training test (Figure S1A). The same results were observed in female mice (Figure S1B). To exclude a possible role of NKT cells, *Rag2*^{-/-} (free from NKT, T, and B cells) and *Rag2*^{-/-}/*γc*^{-/-} mice (free from NKT, T, B, and NK cells) were tested. Similar results were observed in *Rag2*^{-/-}/*γc*^{-/-} mice (Figure 1B), demonstrating an NK cell-specific effect on fear behavior. The *Rag2*^{-/-} mice showed a different fear response compared to C57BL/6 immunoglobulin G (IgG)-treated mice (Figures 1A and 1B), confirming previous evidence of the role of adaptive immune cells in mouse behavior.^{23,24} Since serotonin regulates fear learning and the acquisition of contextual fear memory,^{25,26} we measured its level in the whole hippocampus and found a reduction upon NK cell depletion, while no difference was observed in the prefrontal cortex (PFC), amygdala, or hypothalamus (Figures 1C; S1C, and S1D). To investigate whether this reduction participates in the observed behavioral effects, we treated mice with 5-HTP/benserazide (two intraperitoneal [i.p.] injections, 1 day and 30 min before the test) to reestablish the central serotonin levels (Figure 1C). The data shown in Figure 1D demonstrate that this treatment restored the behavioral responses to the control condition. The behavioral test was performed in parallel in 5-HTP-treated (Figure 1D) and IgG-treated mice (Figure 1A) to compare the different treat-

ments, and two-way ANOVA did not reveal effects among the 5-HTP treatment and IgG groups. Of note, NK cell-dependent serotonin reduction in the hippocampus is not related to variations in the activity of serotonergic neurons in the raphe nuclei (seen as c-Fos staining in aNK1.1-treated mice; Figure S1E), suggesting alternative mechanisms behind these effects. However additional experiments should be employed to exclude changes in serotonin that are not occurring within the CNS.

Platelets regulate serotonin levels in the hippocampus, modulating fear behavior in mice

Platelets are the main body serotonin reserve, and platelet-rich plasma is a putative therapeutic option in inflammation-related neurological diseases.^{27–30} To investigate the hypothesis of a modulatory effect of NK cells on platelet-derived serotonin, and considering that platelets release vesicles as intermediates for cellular communication,^{31,32} we first looked for the presence of PMVs in the healthy mouse brain. We treated mice with a fluorescent anti-GPIbβ Ab (X488) to label platelets and PMV membranes. After 1 h, we collected all microvesicles from the whole-hippocampal, -cortex and -amygdala extracts, demonstrating the presence of fluorescent PMVs in the hippocampus (Figures 2A and S2A), which could represent the mechanism to transfer serotonin to the CNS, but we did not detect PMVs in the cortex or amygdala, consistent with the absence of serotonin reduction in these brain regions (Figure S1D). We then studied the effect of platelet depletion from 2-month-old C57BL/6 mice by i.p. administration of R300 (a mouse anti GPIbα Ab, see scheme in Figure 2B, left, Figure S2B for the efficacy of depletion) on fear learning and memory. Notably, the percentage of freezing upon platelet depletion was considerably higher than that observed in aNK1.1-treated mice (Figure 1A), suggesting additional effects of platelets on neuronal activity. We demonstrated that R300-treated mice showed an increased number of freezing episodes during fear conditioning and contextual fear memory formation, both in male and female mice (Figures 2B and S2C), with no effects on cued fear memory or extinction of memory 5 days after the training (Figure S2D). We then measured the level of serotonin in the whole hippocampus, PFC, amygdala, and hypothalamus and found a hippocampal reduction upon R300 administration with no differences in the other regions (Figures 2C and S2E), similar to the effect of aNK1.1 treatment. Hippocampal serotonin depletion and behavioral effects of R300 were reversed by treating mice (i.p. injection) with 5-HTP/benserazide (Figures 2C and 2D). The behavioral tests shown in Figures 2B and 2D were performed in parallel in the different experimental groups to compare the effect of treatments. Notably, both R300 and aNK1.1 treatments reduced the total amount of microvesicles and PMVs in the hippocampus (Figure S2F), highlighting the role of NK cells in modulating platelet interaction with the brain.

Interestingly, a similar effect on hippocampal serotonin levels was obtained when platelet activity was reduced by treating mice with clopidogrel, which blocks the P2YR12 receptors (Figures 2E, left; and S2G). To exclude possible indirect effects of clopidogrel, we treated platelets isolated *ex vivo* with clopidogrel before re-infusion into the tail vein of mice. After 24 h, the hippocampal serotonin level was measured, and the results

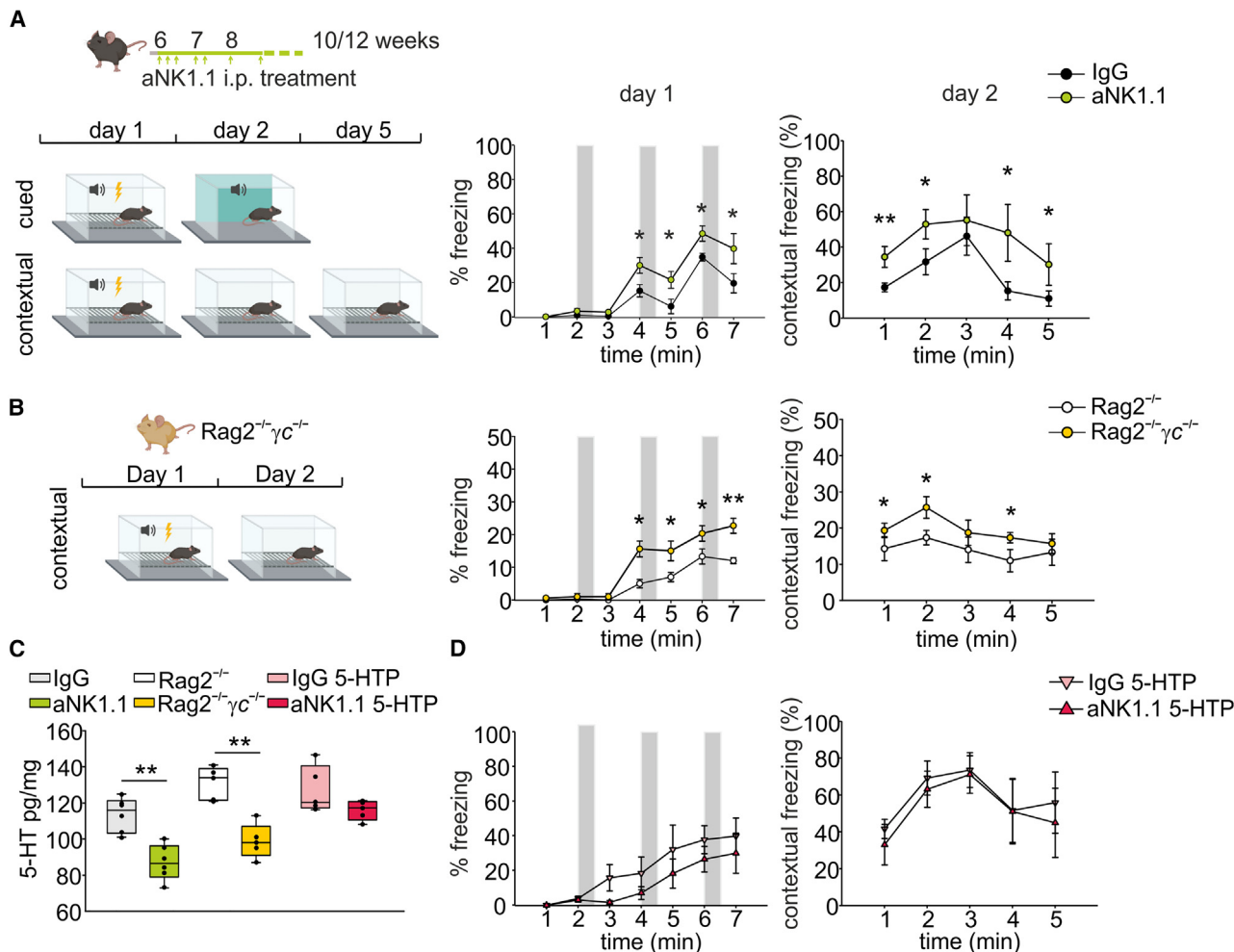


Figure 1. NK cells regulate hippocampal serotonin levels and fear response

(A) Top: Schematic of aNK1.1 treatment in C57BL/6 male mice. Shown are fear responses of IgG- and aNK1.1-treated C57BL/6 mice ($n = 12$ mice per group) during a fear conditioning session on day 1 (gray areas, duration of the conditioned stimulus) (one-way ANOVA, min 4 * $p = 0.023$, min 5 * $p = 0.027$, min 6 * $p = 0.038$, min 7 * $p = 0.034$) and a contextual fear session on day 2 (one-way ANOVA, min 1 ** $p < 0.001$, min 2 * $p = 0.05$, min 4 * $p = 0.039$, min 5 * $p = 0.046$). Results are presented as percent time spent in freezing behavior.

(B) Fear responses of $Rag2^{-/-}$ and $Rag2^{-/-}\gamma c^{-/-}$ mice ($n = 5$ mice per group) during a fear conditioning session on day 1 (one-way ANOVA, min 4 * $p = 0.032$, min 5 * $p = 0.039$, min 6 * $p = 0.040$, min 7 ** $p = 0.003$) and a contextual fear session on day 2 (one-way ANOVA, min 1 * $p = 0.037$, min 2 * $p = 0.043$, min 4 * $p = 0.016$). Results are presented as percent time spent in freezing behavior.

(A and B) Fear conditioning test results for IgG-treated mice vs. $Rag2^{-/-}$ and $Rag2^{-/-}\gamma c^{-/-}$ (** $p < 0.01$ IgG vs. $Rag2^{-/-}$ mice, ** $p < 0.001$ IgG vs. $Rag2^{-/-}\gamma c^{-/-}$ mice, two-way ANOVA). Data are representative of at least three experiments with similar results.

(C) ELISA analysis of 5-HT levels in the hippocampus of IgG- or aNK1.1-treated mice ($n = 6$ per group, ** $p < 0.01$, two tailed Student's t test), $Rag^{-/-}$ or $Rag^{-/-}\gamma c^{-/-}$ mice ($n = 5$ per group, ** $p < 0.01$, two-tailed Student's t test), and IgG- or aNK1.1- and 5HTP-treated mice ($n = 5$ per group). For boxplots, the center line, boxes, and whiskers represent the median, inner quartiles, and rest of the data distribution, respectively.

(D) Fear responses of IgG+5-HTP- or aNK1.1+5-HTP-treated mice ($n = 5$ mice per group) during a fear conditioning session on day 1 and contextual fear session on day 2. Results are presented as percent time spent in freezing behavior.

(Figure 2E, right) showed that it was reduced, confirming a platelet-mediated mechanism. Further, clopidogrel-treated mice showed increased fear learning and contextual memory mimicking the results obtained in platelet-depleted mice (Figure 2F).

To investigate the effect of NK cell depletion on platelet-endothelial cell interaction, two-photon intravital microscopy was used to monitor platelets in the brain vasculature. Platelet number and adhesion in the deep microvessels were analyzed in

control, NK cell-depleted, and clopidogrel-treated mice.^{33,34} The imaged microvasculature received blood flow during recording, and the number of non-adhesive platelets did not differ between treatments (Figures S2H and S2I). Analysis of platelets in microvessels revealed reduced numbers and durations of adhesive events in both NK cell-depleted and clopidogrel-treated mice (Figures 2G–2I), indicating that both treatments affect these interactions.

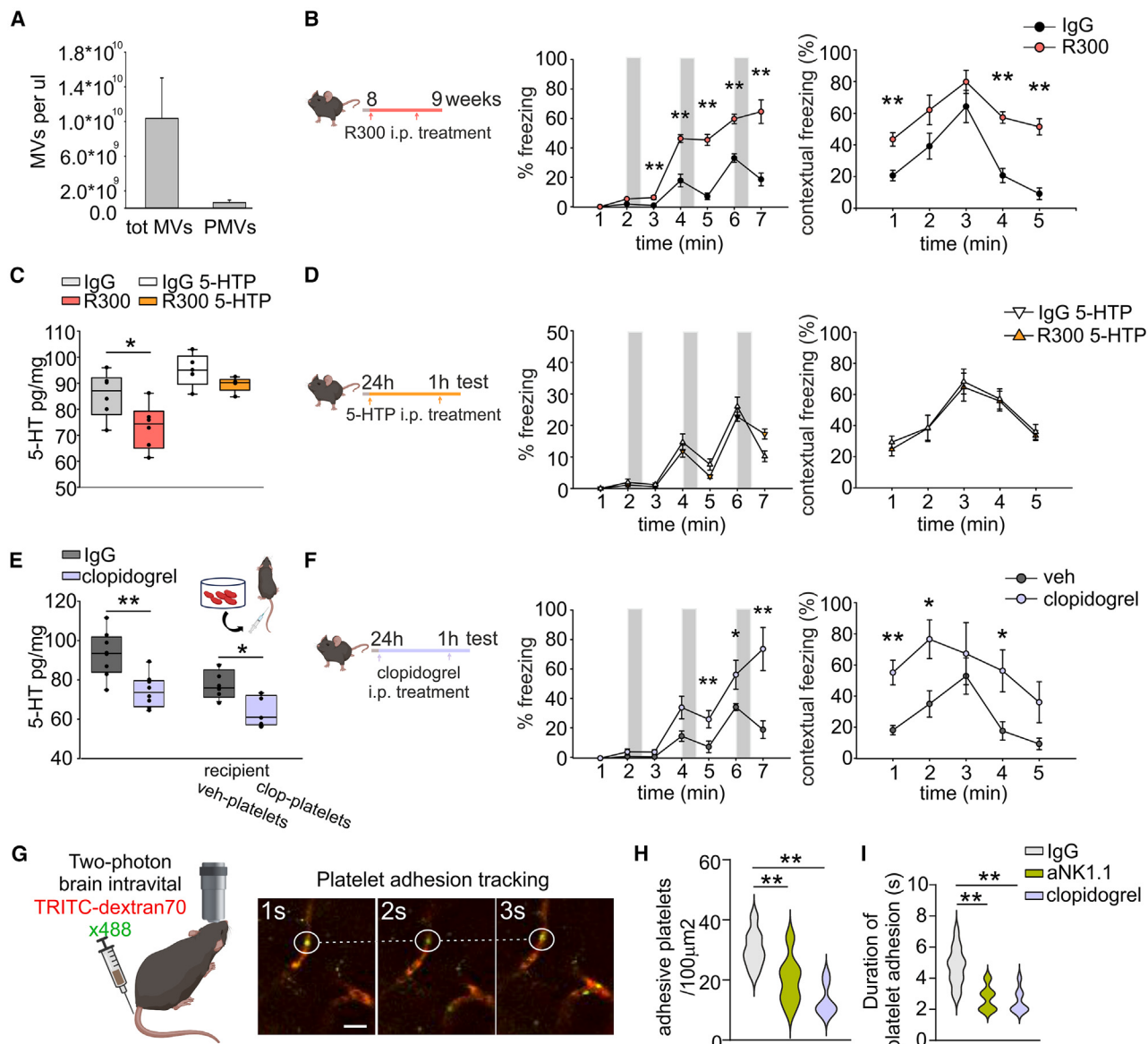


Figure 2. Platelets regulate the freezing behavior in mice

- (A) Analysis of platelet-derived microvesicles (PMVs) marked with X488 antibodies in the hippocampus of C57BL/6 male mice ($n = 5$ mice).
- (B) Left: Schematic of R300 treatment in C57BL/6 male mice. Shown are fear responses of IgG- ($n = 10$) and R300-treated ($n = 7$) mice during a fear conditioning session on day 1 (gray areas, duration of the conditioned stimulus) (one-way ANOVA, $^{**}p < 0.001$) and a contextual fear session on day 2 (one-way ANOVA, $^{**}p < 0.001$). Results are presented as percent of time spent in freezing behavior.
- (C) ELISA analysis of 5-HT levels in the hippocampus of IgG- or R300-treated male mice upon vehicle or 5-HTP administration ($n = 6$ per group, one-way ANOVA, $^{*}p = 0.035$).
- (D) Fear responses of IgG+5-HTP- or R300+5-HTP-treated male mice ($n = 5$ mice per group) during a fear conditioning session on day 1 and contextual fear session on day 2. Results are presented as percent of time spent in freezing behavior.
- (E) ELISA analysis of 5-HT levels in the hippocampus of vehicle- or clopidogrel-treated male mice ($n = 8$ per group, one-way ANOVA, $^{**}p < 0.001$) or of mice infused with platelets pre-treated with clopidogrel *in vitro* (right, $n = 5$ per group, one-way ANOVA, $^{*}p = 0.021$).
- (F) Left: schematic of R300 treatment in C57BL/6 male mice. Shown are fear responses of vehicle- and clopidogrel-treated mice ($n = 8$ per group) during a fear conditioning session on day 1 (one-way ANOVA, min 5 $^{**}p = 0.002$, min 6 $^{*}p = 0.05$, min 7 $^{**}p = 0.006$) and a contextual fear session on day 2 (one-way ANOVA, min 1 $^{**}p < 0.001$, min 2 $^{*}p = 0.033$, min 4 $^{*}p = 0.021$). Results are presented as percent time spent in freezing behavior.
- (G) Images showing the identification of adhesive platelets (circles) compared with the temporary sightings of platelets freely flowing in blood (green) over 3 s, with white dotted lines indicating between-frame platelet tracking.

(legend continued on next page)

NK cells regulate the serotonin load of platelets

Platelets store serotonin in their granules upon uptake in the gastrointestinal (GI) tract through the transporter SERT.³⁵ In the GI tract, serotonin is produced by enterochromaffin cells under the influence of IL-13 released by immune cells, including NK cells.³⁶ To investigate whether NK cells could regulate the serotonin content of platelets through IL-13 in our model, we first measured IL-13 levels in the colon of 2-month-old C57BL/6 mice treated with aNK1.1 and in *Rag2^{-/-}γc^{-/-}* mice, demonstrating a reduction of the level of this cytokine in the colonic segment in the absence of NK cells (Figure 3A). As predicted, aNK1.1 treatment also reduced the serotonin level in the colonic segment (Figure 3B), and the same results were obtained when treating mice with an anti-IL-13 (aIL-13) Ab (Figure 3C). In accordance with our hypothesis, the serotonin content in the platelets of aNK1.1- and aIL-13-treated mice was also reduced (Figure 3D), and platelets isolated from aNK1.1-treated mice had reduced expression of the membrane transporter SERT (Figure 3E). To investigate whether these treatments could affect platelet response to activating stimuli, a number of *ex vivo* experiments were carried out. We described that platelets isolated from aNK1.1-treated mice showed reductions in platelet-immune crosstalk (as evidenced by platelet-leukocyte aggregate [PLA] count) but did not show altered activation in response to ADP stimulation in comparison with IgG-treated mice (Figures 3F, 3G, and S3A). Furthermore, platelets isolated from aNK1.1-treated mice released less serotonin when stimulated with ADP (Figure 3H). These results suggest that NK cell-to-platelet communication selectively affects platelet functions.

To investigate the consequences of these treatments in the CNS, we measured hippocampal 5-HT levels in aIL-13-treated mice; the reduction reported in Figure 3I is compatible with the hypothesis that an impairment of NK cell/IL-13-induced 5-HT production in the colon reduced the platelet cargo of serotonin available for the brain.

Platelets tune the activity of parvalbumin neurons in the hippocampus

Serotonin regulates contextual memory and hippocampal plasticity,³⁷ and brain serotonin deficiency induces exaggerated context-dependent fear memory and shock reactivity, with the involvement of parvalbumin (PV)-inhibitory neurons.^{37–39} To support our hypothesis that a platelet-dependent reduction of hippocampal serotonin mediates the inhibition of hippocampal circuitries, we performed patch-clamp recording from CA1 pyramidal neurons, revealing that R300 treatment reduced the frequency of spontaneous inhibitory postsynaptic currents (sIPSCs) with no changes in current amplitude or kinetics, supporting decreased inhibition upon platelet deprivation (Figure 4A). However, we cannot exclude the involvement of other brain cells, since 5-HT affects 5-HT synthesis in the entire brain.

Then, we analyzed expression of the early gene c-Fos in PV+ neurons in the hippocampal CA1 region of aNK1.1- and R300-treated mice. The data in Figure 4B demonstrate a reduced percentage of c-Fos+ PV neurons in platelet-depleted mice, reversed by 5-HTP treatment (Figure 4B), and increased hippocampal LTP of synaptic transmission, seen as increased amplitude of the field excitatory postsynaptic potentials upon high-frequency stimulation (Figure 4C). In NK cell-depleted mice, we observed a similar reduction of c-Fos staining of hippocampal PV neurons, reversed by 5-HTP treatment (Figure 4D), and increased LTP (Figure 4E). Altogether, these results indicate that NK cell-platelet interaction modulates the inhibitory circuits and hippocampal plasticity.

DISCUSSION

Here, we discovered that NK cells contribute to the gut-platelet-brain dialogue, modulating (1) the production of gut serotonin, (2) the expression level of SERT on the platelet membrane, (3) the platelet serotonin cargo, and (4) the hippocampal serotonin level, and we demonstrated that these effects impact learning and memory of fear behavior in mice. This is a new mechanism of body-to-brain communication that opens a new perspective in understanding the modulation of brain function in physiological and pathological conditions.^{18,19,40}

In different neuropathologies, such as epilepsy, Alzheimer's disease, and traumatic brain injury, platelets enter the CNS and can stimulate neuronal electric activity, leading to an imbalance of excitatory/inhibitory transmission.^{41,42} Further, platelet-secreted factors, such as CXCL4 and the chemokine receptor CXCR3, have beneficial effects on physiological aging.^{18,19,43} In contrast, the mechanism of platelet-brain dialogue in the healthy brain has not yet been investigated. We report that the specific depletion of either NK cells or platelets in mice induced similar neuromodulatory effects on LTP in the hippocampus, with a serotonin-dependent reduction of c-Fos+ PV inhibitory neurons. Our data are consistent with others reporting that serotonin mediates the inhibition of context-dependent aversive memories, reducing LTP in the CA1 region,⁴⁴ and counteracts the consolidation of stressful memories with effects on the tolerance to chronic aversive events through 5-HT1A receptors.⁴⁵ However, we cannot exclude the involvement of additional mechanisms independent of the activation of PV interneurons, such as an interferon γ-mediated modulation of inhibitory neurotransmission^{20,46} or direct crosstalk between platelets and NK cells. In pathological conditions, platelets have been shown to inhibit NK cytotoxic function indirectly by masking malignant cells⁴⁷ and directly by releasing bioactive molecules, such as transforming growth factor β,⁴⁸ or upregulating inhibitory receptors.⁴⁹ However, there is increasing evidence that platelets are necessary to maintain immune homeostasis in healthy

(H) Violin plot of the number of adhesive platelets in the microvessels of IgG-, aNK1.1-, and clopidogrel-treated mice ($n = 3$ per treatment, one-way ANOVA, ** $p < 0.001$).

(I) Adhesive platelet adhesion duration data from each field of brain sampled from IgG-, aNK1.1-, and clopidogrel-treated mice ($n = 12$ acquisitions/3 mice per treatment, one-way ANOVA, ** $p < 0.001$).

For boxplots (C and E), the center line, boxes, and whiskers represent the median, inner quartiles, and rest of the data distribution, respectively. In (B), (D), and (F), data are representative of three experiments with similar results.

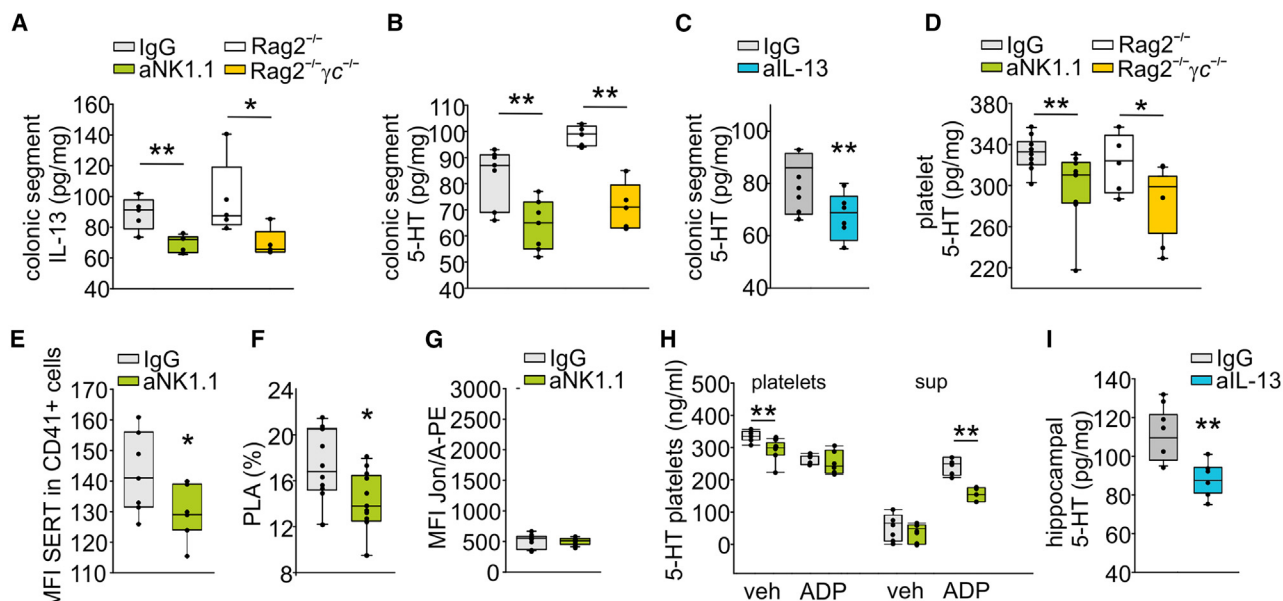


Figure 3. NK cell-platelet dialogue

- (A) ELISA analysis of IL-13 levels in the colonic segment of IgG- or aNK1.1-treated male mice ($n = 5$ per group, one-way ANOVA, $**p < 0.003$) or $Rag2^{-/-}$ and $Rag2^{-/-}\gamma c^{-/-}$ mice ($n = 5$ per group, one-way ANOVA, $*p = 0.032$).
- (B) ELISA analysis of 5-HT levels in the colonic segment of IgG- or aNK1.1-treated male mice ($n = 7$ per group, one-way ANOVA, $**p < 0.005$) or $Rag2^{-/-}$ and $Rag2^{-/-}\gamma c^{-/-}$ mice ($n = 5$ per group, one-way ANOVA, $*p < 0.001$).
- (C) ELISA analysis of 5-HT levels in the colonic segment of IgG- or IL-13-treated mice ($n = 6$ per group, one-way ANOVA, $*p = 0.040$).
- (D) ELISA analysis of 5-HT content in the platelets sorted from IgG- or aNK1.1-treated male mice ($n = 10$ per group, one-way ANOVA, $**p = 0.007$) or $Rag2^{-/-}$ and $Rag2^{-/-}\gamma c^{-/-}$ mice ($n = 5$ per group, one-way ANOVA, $*p = 0.017$).
- (E) Expression of SERT on the surface of platelets (CD41⁺ cells), expressed as median fluorescence intensity (MFI) in mice treated with the NK-depleting Ab or the IgG isotype control ($n = 7$, $*p = 0.021$, Student's t test).
- (F) Quantification of circulating platelet-leukocyte aggregates (PLAs) in whole blood of mice depleted or not of NK cells, measured as the percentage of CD45⁺ leukocytes that were positive for the platelet-specific marker CD41 (unpaired two-tailed t test, $*p = 0.05$).
- (G) Activation of the platelet-specific integrin $\alpha IIb\beta 3$ (JON/A) in untreated whole blood of mice depleted or not of NK cells, expressed as MFI of JON/A-PE, an Ab specific for the active conformation of integrin $\alpha IIb\beta 3$.
- (H) ELISA analysis of 5-HT content in platelets and platelet medium (Supernatant-Sup) sorted from IgG- or aNK1.1-treated mice and stimulated *in vitro* with vehicle or ADP (25 μ M) ($n = 7$ per group, one-way ANOVA, vehicle IgG vs. vehicle aNK1.1, $**p < 0.001$; Sup ADP IgG vs. Sup ADP aNK1.1, $**p = 0.003$).
- (I) ELISA analysis of hippocampal 5-HT levels in IgG- or IL-13-treated mice ($n = 6$ per group, one-way ANOVA, $**p = 0.003$).

For boxplots, the center line, boxes, and whiskers represent the median, inner quartiles, and rest of the data distribution, respectively.

conditions. For instance, in physiological conditions, platelets limit the inflammatory response by interacting with monocytes in a CD47-dependent manner and controlling their metabolic and genetic programs.⁵⁰ Of note, NK cells express high levels of CD47⁵¹ as well as of the ligand of platelet P-selectin (PSGL1),⁵² and platelets store and release sphingosine 1-phosphate, which regulates NK cell trafficking.⁵³ Thus, one could speculate that platelets modulate NK cell function in the steady state. Notably, platelet depletion in mice has a stronger effect on freezing behavior in comparison to NK cell-depleted mice, suggesting additional effects of platelets on neuronal activity.

It is known that, in the CNS, ATP is released by neurons and glial cells during physiological network activity⁵⁴ and rapidly metabolized to ADP, AMP, and adenosine.^{55,56} These purines activate metabotropic and ionotropic receptors, acting as neurotransmitters and neuromodulators.⁵⁷ Our data add platelets as additional elements activated by ADP to release neuroactive molecules, affecting the inhibitory neurotransmission. We show

that clopidogrel, a blocker of the ADP receptor P2Y12, abundantly expressed by platelets,⁵⁸ reduces serotonin levels in the hippocampus. In line with our hypothesis, both platelet depletion and clopidogrel treatment modulated the formation of fear memories in mice. We speculate that release of platelet content in the brain could be also mediated by PMVs because we detected their presence in the hippocampus of healthy mice. Of note, the specific release of molecules stored in vesicles represents a general mechanism for the entry of large molecules through the blood-brain barrier.⁵⁹ The result that NK cell and platelet depletion reduced both serotonin levels and PMVs in the hippocampus, but not in other brain regions, demonstrates a region-specific effect and supports the hypothesis of a possible transfer of serotonin to the brain through PMVs. Further studies are needed to investigate the presence of 5-HT in PMVs that reach the brain. Moreover, intravital imaging experiments provide further evidence that the interaction of platelets with the vascular endothelium relies on NK cells and P2YR12 signaling, suggesting that impairment of this dialogue

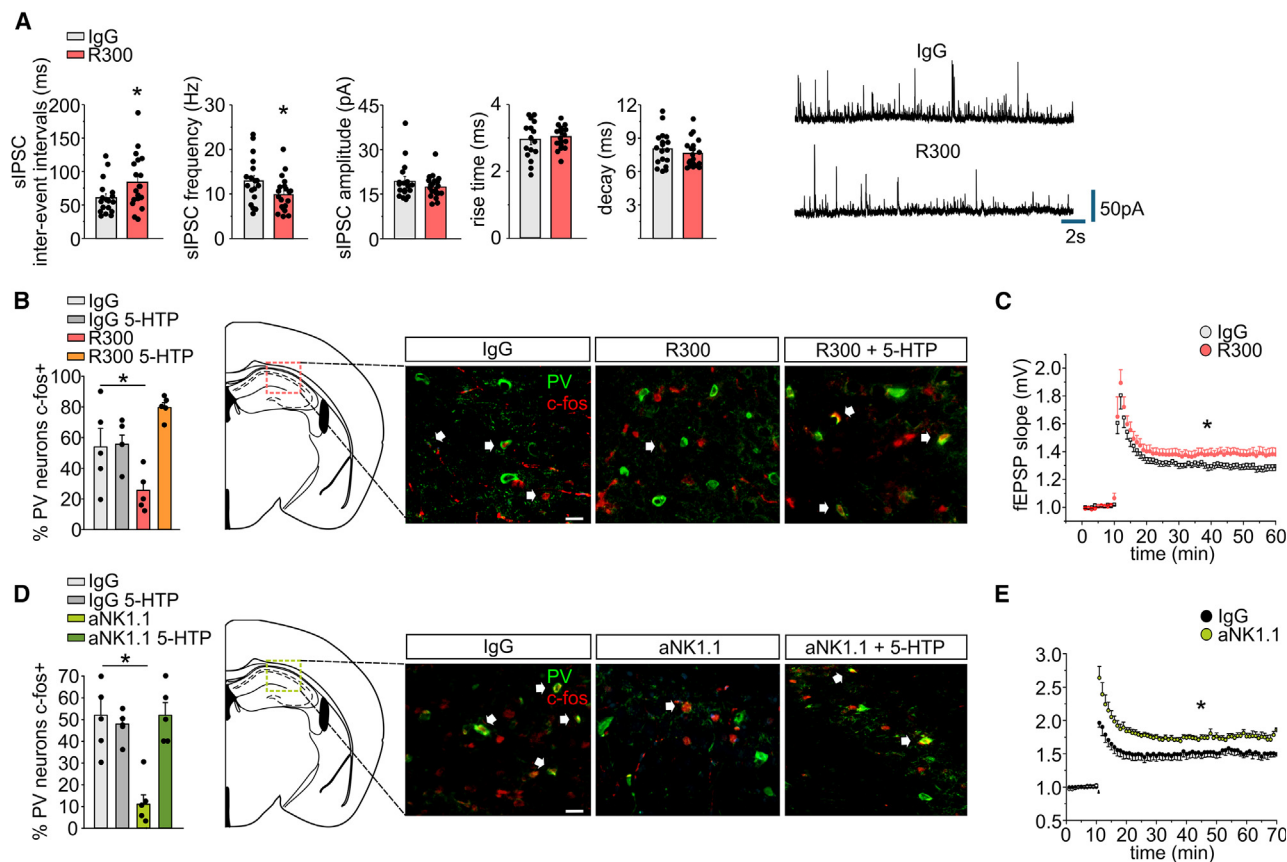


Figure 4. Platelet-derived serotonin modulates inhibitory synaptic transmission in the hippocampus

(A) Bar graphs of inter-event intervals, frequency and amplitude, rise time (rt), and decay time (dt) of sIPSCs recorded from IgG- and R300-treated mice (IgG, 18 cells/4 mice; R300 20 cells/3 mice; one-way ANOVA, * $p = 0.044$). Right: representative traces of sIPSCs recorded in the hippocampal pyramidal neurons obtained from male mice treated with IgG or R300.

(B) Analysis of c-Fos+ PV neurons (indicated by white arrows) in the hippocampus of IgG-, IgG-5-HTP-, R300-, and R300-5-HTP-treated mice, expressed as percentage of total PV neurons ($n = 5$ mice per group, * $p = 0.02$, one-way ANOVA). Representative immunofluorescence is shown on the right. Error bars show mean \pm SEM. Scale bar: 50 μ m.

(C) Field excitatory postsynaptic potential (fEPSP) recorded from the CA1 region of the hippocampus of IgG- or R300-treated mice (IgG, 15 slices/7 mice; R300, 16 slices/6 mice; Student's t test; * $p = 0.05$).

(D) Analysis of c-Fos+ PV neurons (indicated by white arrows) in the hippocampus of IgG-, IgG-5-HTP-, aNK1.1-, and aNK1.1-5-HTP-treated mice, expressed as percentage of total PV neurons ($n = 5$ mice per group, * $p = 0.001$, one-way ANOVA). Representative immunofluorescence is shown on the right. Error bars show mean \pm SEM. Scale bar: 50 μ m.

(E) fEPSP recorded from the CA1 region of the hippocampus of IgG- or aNK1.1-treated mice (IgG, 5 slices/3 mice; aNK1.1, 8 slices/4 mice; Student's t test; * $p = 0.05$).

also affects platelet communication with brain parenchyma. Our experiments, however, cannot exclude indirect mechanisms to increase CNS serotonin from the periphery, such as the gut-brain axis.⁶⁰ Moreover, a better understanding of the mechanisms that allow the entry of PMVs and serotonin across the blood-brain barrier will be necessary to fully support our knowledge of platelet-to-CNS communication under physiological conditions.

Our results also led us to speculate that the depressive syndrome reported in some patients treated with clopidogrel could be due to a reduction of platelet-derived serotonin transfer to the brain, as supported by the beneficial effects of simultaneous treatment with selective serotonin reuptake inhibitors.^{61,62}

To conclude, our data provide a new mechanistic link between platelets and the maintenance of brain homeostasis. Additional studies will be necessary to fully elucidate the potential of these cellular fragments to play physiological roles in gut-neuroimmune communication.

Limitations of the study

We identified a mechanism where NK cells regulate platelet cargo of serotonin that is delivered into the brain, tuning fear memory formation. However, we could not directly prove that platelets release serotonin into the brain, and we cannot exclude an indirect mechanism modulating CNS-derived serotonin. This study also does not provide an explicit link between PV interneuron activity and LTP, and additional experiments would be

required to fully understand the role of PMVs in hippocampal neuronal activity.

RESOURCE AVAILABILITY

Lead contact

Requests for further information, resources, and reagents should be directed to and will be fulfilled by the lead contact, Stefano Garofalo (stefano.garofalo@uniroma1.it).

Materials availability

All unique/stable reagents generated in this study are available from the lead contact with a completed materials transfer agreement.

Data and code availability

- All data reported in this paper will be shared by the lead contact upon request.
- This paper does not report original code.
- Any additional information required to reanalyze the data reported in this paper is available from the [lead contact](#) upon request.

ACKNOWLEDGMENTS

S.G. was supported by NextGenerationEU DD.3175/2021 E DD.3138/2021 CN_3; National Center for Gene Therapy and Drugs based on RNA Technology Codice Progetto CN 00000041; RF GR-2021-12372494; and PRIN 2022 202248875S. C.L. was supported by Progetto ECS 0000024 Rome Technopole-CUP B83C22002820006, PNRR Missione 4 Componente 2 Investimento 1.5, finanziato dall'Unione europea – NextGenerationEU; Seed Sapienza (SP1221842D4094CE); and AIRC IG23010.

AUTHOR CONTRIBUTIONS

S.G. ideated, supervised, and performed most of the experimental work and wrote the article. A.M. and L.Mazzarella contributed to many experimental activities for mouse manipulation. G.Cocozza performed immunofluorescence analysis. A.R extracted and analyzed PMVs from hippocampi. R.P. analyzed PMVs from mouse brains. E.D.P. and M.A.D.C. performed patch-clamp analysis on brain slices. E.D.F. and L.Maggi performed LTP experiments in the CA1 region. G.Chece performed intravital two-photon microscopy surgery in mice. D.I. performed part of the behavioral tests and microdialysis. R.V. and D.A. supervised part of the behavioral tests and microdialysis. R.V. supervised behavioral tests and microdialysis. M.C. supervised PMV experiments. L.S. performed and supervised the *ex vivo* experiments with platelets. C.L. supervised all experimental work and wrote the manuscript.

DECLARATION OF INTERESTS

The authors declare no competing interests.

STAR★METHODS

Detailed methods are provided in the online version of this paper and include the following:

- **KEY RESOURCES TABLE**
- **EXPERIMENTAL MODEL AND STUDY PARTICIPANT DETAILS**
 - Animals
- **METHOD DETAILS**
 - Mice treatment
 - Contextual and cued fear conditioning test
 - MVs extraction and characterization
 - Platelet preparation
 - Measurement of 5-HT by ELISA
 - *In vivo* microdialysis
 - Immunostaining
 - Two photon microscopy analyses

- Hippocampal slices preparation
- **QUANTIFICATION AND STATISTICAL ANALYSIS**

SUPPLEMENTAL INFORMATION

Supplemental information can be found online at <https://doi.org/10.1016/j.celrep.2025.115261>.

Received: July 3, 2024

Revised: November 13, 2024

Accepted: January 13, 2025

Published: February 3, 2025

REFERENCES

1. Ordovas-Montanes, J., Rakoff-Nahoum, S., Huang, S., Riol-Blanco, L., Barreiro, O., and von Andrian, U.H. (2015). The Regulation of Immunological Processes by Peripheral Neurons in Homeostasis and Disease. *Trends Immunol.* 36, 578–604. <https://doi.org/10.1016/j.it.2015.08.007>.
2. Mrdjen, D., Pavlovic, A., Hartmann, F.J., Schreiner, B., Utz, S.G., Leung, B.P., Lelios, I., Heppner, F.L., Kipnis, J., Merkler, D., et al. (2018). High-Dimensional Single-Cell Mapping of Central Nervous System Immune Cells Reveals Distinct Myeloid Subsets in Health, Aging, and Disease. *Immunity* 48, 599. <https://doi.org/10.1016/j.immuni.2018.02.014>.
3. Brynskikh, A., Warren, T., Zhu, J., and Kipnis, J. (2008). Adaptive immunity affects learning behavior in mice. *Brain Behav. Immun.* 22, 861–869. <https://doi.org/10.1016/j.bbi.2007.12.008>.
4. Kipnis, J., Avidan, H., Caspi, R.R., and Schwartz, M. (2004). Dual effect of CD4+CD25+ regulatory T cells in neurodegeneration: a dialogue with microglia. *Proc. Natl. Acad. Sci. USA* 101, 14663–14669. <https://doi.org/10.1073/pnas.0404842101>.
5. Wolf, S.A., Steiner, B., Akpinarli, A., Kammertoens, T., Nassenstein, C., Braun, A., Blankenstein, T., and Kempermann, G. (2009). CD4-positive T lymphocytes provide a neuroimmunological link in the control of adult hippocampal neurogenesis. *J. Immunol.* 182, 3979–3984. <https://doi.org/10.4049/jimmunol.0801218>.
6. Leiter, O., and Walker, T.L. (2019). Platelets: The missing link between the blood and brain? *Prog. Neurobiol.* 183, 101695. <https://doi.org/10.1016/j.pneurobio.2019.101695>.
7. Kapur, R., and Semple, J.W. (2016). Platelets as immune-sensing cells. *Blood Adv.* 1, 10–14. <https://doi.org/10.1182/bloodadvances.2016000067>.
8. Kapur, R., Zufferey, A., Boilard, E., and Semple, J.W. (2015). Nouvelle cuisine: platelets served with inflammation. *J. Immunol.*, 5579–5587. <https://doi.org/10.4049/jimmunol.1500259>.
9. Eriksson, O., Mohlin, C., Nilsson, B., and Ekdahl, K.N. (2019). The Human Platelet as an Innate Immune Cell: Interactions Between Activated Platelets and the Complement System. *Front. Immunol.* 10, 1590. <https://doi.org/10.3389/fimmu.2019.01590>.
10. Milioli, M., Ibáñez-Vea, M., Sidoli, S., Palmisano, G., Careri, M., and Larsen, M.R. (2015). Quantitative proteomics analysis of platelet-derived microparticles reveals distinct protein signatures when stimulated by different physiological agonists. *J. Proteomics* 121, 56–66. <https://doi.org/10.1016/j.jprot.2015.03.013>.
11. Adnot, S., Houssaini, A., Abid, S., Marcos, E., and Amsellem, V. (2013). Serotonin transporter and serotonin receptors. *Handb. Exp. Pharmacol.* 218, 365–380. https://doi.org/10.1007/978-3-642-38664-0_15.
12. Zhang, X., Beaulieu, J.-M., Sotnikova, T.D., Gainetdinov, R.R., and Caron, M.G. (2004). Tryptophan hydroxylase-2 controls brain serotonin synthesis. *Science* 305, 217. <https://doi.org/10.1126/science.1097540>.
13. Shoji, H., Ikeda, K., and Miyakawa, T. (2023). Behavioral phenotype, intestinal microbiome, and brain neuronal activity of male serotonin transporter knockout mice. *Mol. Brain* 16, 32. <https://doi.org/10.1186/s13041-023-01020-2>.

14. Kazanis, I., Feichtner, M., Lange, S., Rotheneichner, P., Hainzl, S., Öller, M., Schallmoser, K., Rohde, E., Reitsamer, H.A., Couillard-Despres, S., et al. (2015). Lesion-induced accumulation of platelets promotes survival of adult neural stem/progenitor cells. *Exp. Neurol.* 269, 75–89. <https://doi.org/10.1016/j.expneurol.2015.03.018>.
15. Hayon, Y., Dashevsky, O., Shai, E., Varon, D., and Leker, R.R. (2012). Platelet microparticles promote neural stem cell proliferation, survival and differentiation. *J. Mol. Neurosci.* 47, 659–665. <https://doi.org/10.1007/s12031-012-9711-y>.
16. Behari, M., and Srivastava, M. (2013). Role of platelets in neurodegenerative diseases: a universal pathophysiology. *Int. J. Neurosci.* 123, 287–299. <https://doi.org/10.3109/00207454.2012.751534>.
17. Piven, J., Tsai, G.C., Nehme, E., Coyle, J.T., Chase, G.A., and Folstein, S.E. (1991). Platelet serotonin, a possible marker for familial autism. *J. Autism Dev. Disord.* 21, 51–59. <https://doi.org/10.1007/BF02206997>.
18. Leiter, O., Brici, D., Fletcher, S.J., Yong, X.L.H., Widagdo, J., Matigian, N., Schroer, A.B., Bieri, G., Blackmore, D.G., Bartlett, P.F., et al. (2023). Platelet-derived exosome CXCL4/platelet factor 4 rejuvenates hippocampal neurogenesis and restores cognitive function in aged mice. *Nat. Commun.* 14, 4375. <https://doi.org/10.1038/s41467-023-39873-9>.
19. Schroer, A.B., Ventura, P.B., Sucharov, J., Misra, R., Chui, M.K.K., Bieri, G., Horowitz, A.M., Smith, L.K., Encabo, K., Tenggara, I., et al. (2023). Platelet factors attenuate inflammation and rescue cognition in ageing. *Nature* 620, 1071–1079. <https://doi.org/10.1038/s41586-023-06436-3>.
20. Garofalo, S., Cocozza, G., Mormino, A., Bernardini, G., Russo, E., Ielpo, D., Andolina, D., Ventura, R., Martinello, K., Renzi, M., et al. (2023). Natural killer cells and innate lymphoid cells 1 tune anxiety-like behavior and memory in mice via interferon-γ and acetylcholine. *Nat. Commun.* 14, 3103. <https://doi.org/10.1038/s41467-023-38899-3>.
21. Aibar, S., González-Blas, C.B., Moerman, T., Huynh-Thu, V.A., Imrichova, H., Hulselmans, G., Rambow, F., Marine, J.-C., Geurts, P., Aerts, J., et al. (2017). SCENIC: single-cell regulatory network inference and clustering. *Nat. Methods* 14, 1083–1086. <https://doi.org/10.1038/nmeth.4463>.
22. Garofalo, S., Porzia, A., Mainiero, F., Di Angelantonio, S., Cortese, B., Basilio, B., Pagani, F., Cignitti, G., Chece, G., Maggio, R., et al. (2017). Environmental stimuli shape microglial plasticity in glioma. *eLife* 6, e33415. <https://doi.org/10.7554/eLife.33415>.
23. McCusker, R.H., and Kelley, K.W. (2013). Immune-neural connections: how the immune system's response to infectious agents influences behavior. *J. Exp. Biol.* 216, 84–98. <https://doi.org/10.1242/jeb.073411>.
24. Kipnis, J., Cohen, H., Cardon, M., Ziv, Y., and Schwartz, M. (2004). T cell deficiency leads to cognitive dysfunction: implications for therapeutic vaccination for schizophrenia and other psychiatric conditions. *Proc. Natl. Acad. Sci. USA* 101, 8180–8185. <https://doi.org/10.1073/pnas.0402268101>.
25. Lacagnina, A.F., Brockway, E.T., Crovetti, C.R., Shue, F., McCarty, M.J., Sattler, K.P., Lim, S.C., Santos, S.L., Denny, C.A., and Drew, M.R. (2019). Distinct hippocampal engrams control extinction and relapse of fear memory. *Nat. Neurosci.* 22, 753–761. <https://doi.org/10.1038/s41593-019-0361-z>.
26. Gutknecht, L., Popp, S., Waider, J., Sommerlandt, F.M.J., Göppner, C., Post, A., Reif, A., van den Hove, D., Strelakova, T., Schmitt, A., et al. (2015). Interaction of brain 5-HT synthesis deficiency, chronic stress and sex differentially impact emotional behavior in Tph2 knockout mice. *Psychopharmacology* 232, 2429–2441. <https://doi.org/10.1007/s00213-015-3879-0>.
27. Bayat, M., Zabihi, S., Karbalaei, N., and Haghani, M. (2020). Time-dependent effects of platelet-rich plasma on the memory and hippocampal synaptic plasticity impairment in vascular dementia induced by chronic cerebral hypoperfusion. *Brain Res. Bull.* 164, 299–306. <https://doi.org/10.1016/j.brainresbull.2020.08.033>.
28. Borhani-Haghghi, M., and Mohamadi, Y. (2019). The therapeutic effect of platelet-rich plasma on the experimental autoimmune encephalomyelitis mice. *J. Neuroimmunol.* 333, 476958. <https://doi.org/10.1016/j.jneuroim.2019.04.018>.
29. Anitua, E., Pascual, C., Antequera, D., Bolos, M., Padilla, S., Orive, G., and Carro, E. (2014). Plasma rich in growth factors (PRGF-Endoret) reduces neuropathologic hallmarks and improves cognitive functions in an Alzheimer's disease mouse model. *Neurobiol. Aging* 35, 1582–1595. <https://doi.org/10.1016/j.neurobiolaging.2014.01.009>.
30. Anitua, E., Pascual, C., Pérez-Gonzalez, R., Orive, G., and Carro, E. (2015). Intranasal PRGF-Endoret enhances neuronal survival and attenuates NF-κB-dependent inflammation process in a mouse model of Parkinson's disease. *J. Contr. Release* 203, 170–180. <https://doi.org/10.1016/j.jconrel.2015.02.030>.
31. Puhm, F., Boilard, E., and Machlus, K.R. (2021). Platelet Extracellular Vesicles: Beyond the Blood. *Arterioscler. Thromb. Vasc. Biol.* 41, 87–96. <https://doi.org/10.1161/ATVBAHA.120.314644>.
32. Mabrouk, M., Guessous, F., Naya, A., Merhi, Y., and Zaid, Y. (2023). The Pathophysiological Role of Platelet-Derived Extracellular Vesicles. *Semin. Thromb. Hemost.* 49, 279–283. <https://doi.org/10.1055/s-0042-1756705>.
33. Shih, A.Y., Driscoll, J.D., Drew, P.J., Nishimura, N., Schaffer, C.B., and Kleinfeld, D. (2012). Two-photon microscopy as a tool to study blood flow and neurovascular coupling in the rodent brain. *J. Cerebr. Blood Flow Metabol.* 32, 1277–1309. <https://doi.org/10.1038/jcbfm.2011.196>.
34. Cleary, S.J., Hobbs, C., Amison, R.T., Arnold, S., O'Shaughnessy, B.G., Lefrançais, E., Mallavia, B., Looney, M.R., Page, C.P., and Pitchford, S.C. (2019). LPS-induced Lung Platelet Recruitment Occurs Independently from Neutrophils, PSGL-1, and P-Selectin. *Am. J. Respir. Cell Mol. Biol.* 61, 232–243. <https://doi.org/10.1165/rcmb.2018-0182OC>.
35. Koopman, N., Katsavavis, D., Hove, A.S.T., Brul, S., Jonge, W.J.d., and Seppen, J. (2021). The Multifaceted Role of Serotonin in Intestinal Homeostasis. *Int. J. Mol. Sci.* 22, 9487. <https://doi.org/10.3390/ijms22179487>.
36. Shahib, M.S., Wang, H., Kim, J.J., Sunjic, I., Ghia, J.-E., Denou, E., Collins, M., Denburg, J.A., and Khan, W.I. (2013). Interleukin 13 and serotonin: linking the immune and endocrine systems in murine models of intestinal inflammation. *PLoS One* 8, e72774. <https://doi.org/10.1371/journal.pone.0072774>.
37. Waider, J., Popp, S., Mlinar, B., Montalbano, A., Bonfiglio, F., Aboagye, B., Thuy, E., Kern, R., Thiel, C., Araragi, N., et al. (2019). Serotonin Deficiency Increases Context-Dependent Fear Learning Through Modulation of Hippocampal Activity. *Front. Neurosci.* 13, 245. <https://doi.org/10.3389/fnins.2019.00245>.
38. Tzilivaki, A., Tukker, J.J., Maier, N., Poirazi, P., Sammons, R.P., and Schmitz, D. (2023). Hippocampal GABAergic interneurons and memory. *Neuron* 111, 3154–3175. <https://doi.org/10.1016/j.neuron.2023.06.016>.
39. Ognjanovski, N., Schaeffer, S., Wu, J., Mofakham, S., Maruyama, D., Zochowski, M., and Aton, S.J. (2017). Erratum: Parvalbumin-expressing interneurons coordinate hippocampal network dynamics required for memory consolidation. *Nat. Commun.* 8, 16120. <https://doi.org/10.1038/ncomms16120>.
40. Marrocco, F., Delli Carpini, M., Garofalo, S., Giampaoli, O., De Felice, E., Di Castro, M.A., Maggi, L., Scavizzi, F., Raspa, M., Marini, F., et al. (2022). Short-chain fatty acids promote the effect of environmental signals on the gut microbiome and metabolome in mice. *Commun. Biol.* 5, 517. <https://doi.org/10.1038/s42003-022-03468-9>.
41. Kumar, M.A. (2013). Coagulopathy associated with traumatic brain injury. *Curr. Neurol. Neurosci. Rep.* 13, 391. <https://doi.org/10.1007/s11910-013-0391-y>.
42. Musto, A.E., Rosencrans, R.F., Walker, C.P., Bhattacharjee, S., Raulji, C.M., Belyayev, L., Fang, Z., Gordon, W.C., and Bazan, N.G. (2016). Dysfunctional epileptic neuronal circuits and dysmorphic dendritic spines are mitigated by platelet-activating factor receptor antagonism. *Sci. Rep.* 6, 30298. <https://doi.org/10.1038/srep30298>.
43. Park, C., Hahn, O., Gupta, S., Moreno, A.J., Marino, F., Kedir, B., Wang, D., Villeda, S.A., Wyss-Coray, T., and Dubal, D.B. (2023). Platelet factors

- are induced by longevity factor klotho and enhance cognition in young and aging mice. *Nat. Aging* 3, 1067–1078. <https://doi.org/10.1038/s43587-023-00468-0>.
44. Mlinar, B., Stocca, G., and Corradetti, R. (2015). Endogenous serotonin facilitates hippocampal long-term potentiation at CA3/CA1 synapses. *J. Neural. Transm.* 122, 177–185. <https://doi.org/10.1007/s00702-014-1246-7>.
 45. Graeff, F.G., Guimarães, F.S., De Andrade, T.G., and Deakin, J.F. (1996). Role of 5-HT in stress, anxiety, and depression. *Pharmacol. Biochem. Behav.* 54, 129–141. [https://doi.org/10.1016/0091-3057\(95\)02135-3](https://doi.org/10.1016/0091-3057(95)02135-3).
 46. Filiano, A.J., Xu, Y., Tustison, N.J., Marsh, R.L., Baker, W., Smirnov, I., Overall, C.C., Gadani, S.P., Turner, S.D., Weng, Z., et al. (2016). Unexpected role of interferon- γ in regulating neuronal connectivity and social behaviour. *Nature* 535, 425–429. <https://doi.org/10.1038/nature18626>.
 47. Nieswandt, B., Hafner, M., Echtenacher, B., and Männel, D.N. (1999). Lysis of tumor cells by natural killer cells in mice is impeded by platelets. *Cancer Res.* 59, 1295–1300.
 48. Du, Y., Liu, X., and Guo, S.-W. (2017). Platelets impair natural killer cell reactivity and function in endometriosis through multiple mechanisms. *Hum. Reprod.* 32, 794–810. <https://doi.org/10.1093/humrep/dex014>.
 49. Clar, K.L., Hinterleitner, C., Schneider, P., Salih, H.R., and Maurer, S. (2019). Inhibition of NK Reactivity Against Solid Tumors by Platelet-Derived RANKL. *Cancers* 11, 277. <https://doi.org/10.3390/cancers11030277>.
 50. Li, C., Ture, S.K., Nieves-Lopez, B., Blick-Nitko, S.K., Maurya, P., Livada, A.C., Stahl, T.J., Kim, M., Pietropaoli, A.P., and Morrell, C.N. (2024). Thrombocytopenia Independently Leads to Changes in Monocyte Immune Function. *Circ. Res.* 134, 970–986. <https://doi.org/10.1161/CIRCRESAHA.123.323662>.
 51. Nath, P.R., Gangaplara, A., Pal-Nath, D., Mandal, A., Maric, D., Sipes, J.M., Cam, M., Shevach, E.M., and Roberts, D.D. (2018). CD47 Expression in Natural Killer Cells Regulates Homeostasis and Modulates Immune Response to Lymphocytic Choriomeningitis Virus. *Front. Immunol.* 9, 2985. <https://doi.org/10.3389/fimmu.2018.02985>.
 52. Laszik, Z., Jansen, P.J., Cummings, R.D., Tedder, T.F., McEver, R.P., and Moore, K.L. (1996). P-selectin glycoprotein ligand-1 is broadly expressed in cells of myeloid, lymphoid, and dendritic lineage and in some nonhematopoietic cells. *Blood* 88, 3010–3021. <https://doi.org/10.1182/blood.V88.8.3010.bloodjournal8883010>.
 53. Vivier, E., Tomasello, E., Baratin, M., Walzer, T., and Ugolini, S. (2008). Functions of natural killer cells. *Nat. Immunol.* 9, 503–510. <https://doi.org/10.1038/ni1582>.
 54. Schulz, S.B., Klaft, Z.-J., Rösler, A.R., Heinemann, U., and Gerevich, Z. (2012). Purinergic P2X, P2Y and adenosine receptors differentially modulate hippocampal gamma oscillations. *Neuropharmacology* 62, 914–924. <https://doi.org/10.1016/j.neuropharm.2011.09.024>.
 55. Shigetomi, E., Sakai, K., and Koizumi, S. (2023). Extracellular ATP/adenosine dynamics in the brain and its role in health and disease. *Front. Cell Dev. Biol.* 11, 1343653. <https://doi.org/10.3389/fcell.2023.1343653>.
 56. Dale, N. (2021). Real-time measurement of adenosine and ATP release in the central nervous system. *Purinergic Signal.* 17, 109–115. <https://doi.org/10.1007/s11302-020-09733-y>.
 57. Abbracchio, M.P., Burnstock, G., Verkhratsky, A., and Zimmermann, H. (2009). Purinergic signalling in the nervous system: an overview. *Trends Neurosci.* 32, 19–29. <https://doi.org/10.1016/j.tins.2008.10.001>.
 58. Sangkuhl, K., Klein, T.E., and Altman, R.B. (2010). Clopidogrel pathway. *Pharmacogenetics Genom.* 20, 463–465. <https://doi.org/10.1097/FPC.0b013e3283385420>.
 59. Busatto, S., Morad, G., Guo, P., and Moses, M.A. (2021). The role of extracellular vesicles in the physiological and pathological regulation of the blood-brain barrier. *FASEB Biadv.* 3, 665–675. <https://doi.org/10.1096/fba.2021-00045>.
 60. Qu, S., Yu, Z., Zhou, Y., Wang, S., Jia, M., Chen, T., and Zhang, X. (2024). Gut microbiota modulates neurotransmitter and gut-brain signaling. *Microbiol. Res.* 287, 127858. <https://doi.org/10.1016/j.micres.2024.127858>.
 61. Bykov, K., Schneeweiss, S., Donneyong, M.M., Dong, Y.-H., Choudhry, N.K., and Gagne, J.J. (2017). Impact of an Interaction Between Clopidogrel and Selective Serotonin Reuptake Inhibitors. *Am. J. Cardiol.* 119, 651–657. <https://doi.org/10.1016/j.amjcard.2016.10.052>.
 62. Zafar, M.U., Paz-Yepes, M., Shimbo, D., Vilahur, G., Burg, M.M., Chaplin, W., Fuster, V., Davidson, K.W., and Badimon, J.J. (2010). Anxiety is a better predictor of platelet reactivity in coronary artery disease patients than depression. *Eur. Heart J.* 31, 1573–1582. <https://doi.org/10.1093/euroheartj/ehp602>.
 63. Da, Q., Derry, P.J., Lam, F.W., and Rumbaut, R.E. (2018). Fluorescent labeling of endogenous platelets for intravital microscopy: Effects on platelet function. *Microcirculation* 25, e12457. <https://doi.org/10.1111/micc.12457>.
 64. Grill, A., Kiouptsi, K., Karwot, C., Jurk, K., and Reinhardt, C. (2020). Evaluation of blood collection methods and anticoagulants for platelet function analyses on C57BL/6J laboratory mice. *Platelets* 31, 981–988. <https://doi.org/10.1080/09537104.2019.1701185>.
 65. Di Chiara, G., Tanda, G., Frau, R., and Carboni, E. (1993). On the preferential release of dopamine in the nucleus accumbens by amphetamine: further evidence obtained by vertically implanted concentric dialysis probes. *Psychopharmacology* 112, 398–402. <https://doi.org/10.1007/BF02244939>.

STAR★METHODS

KEY RESOURCES TABLE

REAGENT or RESOURCE	SOURCE	IDENTIFIER
Antibodies		
Anti-NK1.1	Bioxcell	Cat#BE0036, RRID:AB_1107737
anti-c-fos [2H2]	Abcam	Cat# ab208942 RRID:AB_2747772
Anti-Serotonin	Immunostar	RRID:AB_572263
R300	Emfret analytics	RRID:AB_2721041
DyLight 488-conjugated anti-mouse GP Ib β antibody (x-488)	Emfret analytics	RRID:AB_2890921
Anti-mIL-13	Invivogen	RRID:AB_2722583
Anti-Serotonin Transporter (SERT) (extracellular)-FITC Antibody	Alomone Labs	RRID:AB_2925082
CD115 (c-fms) Monoclonal Antibody (), Alexa Fluor 488	eBioscience™	Cat# AFS98
Hoechst 33342	Invitrogen	Cat# H3570, RRID:AB_10626776
CD11b Monoclonal Antibody (M1/70), PE	eBioscience™	Cat# 12-0112-82
CD45 Monoclonal Antibody (30-F11), PerCP-Cyanine5.5	eBioscience™	Catalog # 45-0451-82
CD41a Monoclonal Antibody (eBioMWReg30 (MWReg30), APC	Invitrogen	Catalog # 17-0411-82
Ly-6G Monoclonal Antibody (1A8-Ly6g), PE	eBioscience™	Catalog # 12-9668-82
Chemicals, peptides, and recombinant proteins		
5-HTP/benserazide	Merck	Cat# H9772
Clopidogrel	Sigma-Aldrich	Cat# s-c0614
Goat Serum	GIBCO Invitrogen	Cat# 16210-064
PBS tablets	Sigma-Aldrich	Cat# P4417
Citric acid based antigen unmasking solution	Vector Laboratories	Cat# H-3300
Critical commercial assays		
ELISA mouse IL-13	GIBCO Invitrogen	BMS6015
ELISA serotonin	Abcam	ab133053
Experimental models: Organisms/strains		
C57BL/6NCrl	Charles River	RRID:MGI:2683688
Software and algorithms		
SigmaPlot v 11.0	Systat Software Inc.	https://systatsoftware.com
ImageJ	National Institute of Health	https://imagej.net/ij
Metamorph v 7.6.5.0	Molecular Devices	https://www.moleculardevices.com
Corel Draw v 20.0, v 25.0	Corel Corporation	https://www.coreldraw.com
ZetaView software (version 8.05.16 SP3)	-	-
FlowJo software	-	-
Software control	Prairie View Imaging, Bruker	-
pClamp 10 software	Axon Instruments	-
MiniAnalysis software	Synaptosoft Fort Lee	-
Other		
Control AIN-76A diet	Research Diets	Cat# D10001i

EXPERIMENTAL MODEL AND STUDY PARTICIPANT DETAILS

Animals

Experiments described in the present work were approved by the Animal Welfare Body of Sapienza University and the Italian Ministry of Health (authorization n° 775/2020-PR; n° 356/2023-PR; n° 631/2022-PR) in accordance with the guidelines on the ethical use of animals from the European Community Council Directive of September 22, 2010 (2010/63/EU), and from the Italian D.Leg 26/2014. All possible efforts were made to minimize animal suffering, and to reduce the number of animals used per condition by calculating the

necessary sample size before performing the experiments. All studies were performed using adult male and female mice at the indicated ages. Male mice data are reported in the main figures, female experiments are reported in the supplementary information. C57BL/6J, Rag $2^{-/-}$ (B6.Cg-Rag2tm1.1Cgn/J, RRID:IMSR_JAX:008449), Rag $2^{-/-}\gamma c^{-/-}$ (C; 129S4-Rag2tm1.1Flv II2rgtm1.1Flv/J, RRID:IMSR_JAX:014593) mice (C57BL/6 background) were obtained from Jackson Laboratory (Bar Harbor, ME, USA) and from Charles River (Calco, Italy). Mice were housed in standard breeding cages at constant temperature ($22 \pm 1^\circ\text{C}$) and relative humidity (50%), with a 12:12 h light:dark cycle (light on 07.00–19.00 h). Food and water were available *ad libitum*. Microbiological analyses were routinely (each 3–4 months) performed and defined endemic Norovirus in our conventional animal facility.

METHOD DETAILS

Mice treatment

Starting at 6 weeks of age, C57BL/6 mice were randomly grouped for the treatments. NK cell depletion was performed using a blocking Ab against NK1.1, which recognizes an epitope of the NKR1Pc activating receptor (PK136). Mice were intraperitoneal (i.p.) injected i.p. with 200 µg (in 100 µL) of anti-NK1.1 Ab every 2 days the first week, every 4 days the second week and then repeated once a week until the age described in the text, at least three weeks. NK cell depletion was monitored by FACS. For platelet depletion and IL-13 blockade, 8-week-old mice were treated with R300 (2 µg/g) or AbIL-13 (4 mg/kg) respectively, by i.p. injection repeated every 4 days for 1 week. The platelet depletion was about 99% (see Extended Figure 2A). For each experiment, control mice were treated with the corresponding control IgG, with no differences between untreated wild type and IgG-treated wild type mice. For Clopidogrel (20 mg/kg) treatment, 8-week-old mice were i.p. treated 1 day and 30min before the experiments. To increase the serotonin levels specifically in the brain, mice were injected intraperitoneally (i.p.) with two 10 mg/kg doses of 5-HTP (H9772, Sigma-Aldrich), in combination with 12.5 mg/kg benserazide (B7283, Sigma-Aldrich; a peripheral decarboxylase inhibitor) 1 day and 30min before the behavioral tests. To target *in vivo* the platelet, DyLight 488-conjugated anti-mouse GP Ib β antibody (x-488) (10 µg per mouse) was intravenous (i.v.) administrated. The maximum fluorescence peak of the platelets is obtained after 15 min.⁶³

Contextual and cued fear conditioning test

Experimental groups were blinded and randomly assigned before the start of behavioral experiments and remained blinded until all data were collected. Mice were tested at 10–12 weeks of age. Sample sizes were chosen on the basis of a power analysis using estimates from previously published experiments. Before all experiments, mice were transported to the behavior room and left at least 30 min to habituate. Individual mice were placed in a test chamber (UGO BASILE) and received three pairings of conditioned stimulus (30 s of white noise at 55 dB) and unconditioned stimulus (interstimulus interval, 1.5 min) for fear conditioning. Conditioned stimulus terminated together with a foot shock (2 s and 0.35 mA). 24 h after conditioning each mouse was placed again in the same chamber without any stimuli for 5 min, for the contextual test. 1–2 h later, the cued test was performed modifying the chamber walls with different design. Each mouse was habituated to the chamber over a period of 180 s before presentation with continued conditioned stimulus for additional 180 s.

MVs extraction and characterization

Platelets were targeted with intravenous injection of anti-GP Ib β antibody (X488) conjugated with green 488 fluorophore. Hippocampal, cortex and amygdala lysates (same amount of tissue for all brain areas) from X488-treated mice were collected and centrifuged at 1200 × g for 5 min to remove cell debris. Then, the supernatant was centrifuged at 10000 × g for 30 min at 4°C. The resulting pellet, containing microvesicles (MVs) mean size 278.5 ± 99.4 nm, was re-suspended in a 0.22 µm filtered PBS (Thermo Fisher Scientific, Waltham, MA, USA) to a final volume of 1 mL. The dimension and concentration of MVs were determined using nanoparticle tracking analyzer (ZetaView PMX-130, Particle Metrix, Meerbusch, Germany). The analysis was performed in scatter mode with a 488 nm laser wavelength to identify the PMVs with the following settings: minimum brightness 30; minimum area 10; maximum area 1000; temperature 20.03°C; shutter 100. ZetaView software (version 8.05.16 SP3) was used for the analysis of light scattering at 11 camera positions to determine the size profiling and quantification of PMVs.

Platelet preparation

Blood was drawn from the retro-orbital plexus into heparinized tubes with capillaries pre-treated with heparin.⁶⁴ Platelet-rich plasma (PRP) was obtained by centrifugation at 100g for 5 min. PRP was centrifuged at 700g in the presence of PGI₂ (5 µM) for 5 min at room temperature. After two washing steps, pelleted platelets were resuspended in modified Tyrode's buffer (137 mM NaCl, 0.3 mM Na₂HPO₄, 2 mM KCl, 12 mM NaHCO₃, 5 mM N-2-hydroxyethylpiperazine-N'-2-ethanesulfonic acid, 5 mM glucose, pH 7.3) containing 1 mM CaCl₂.

Platelet count

Mice were bled retro-orbitally (50 µL) in heparinized tubes and platelets were labeled for 15 min with 2 µg/ml APC-labeled antibody to CD41a (eBioscience). Samples were diluted with PBS and the number of CD41a-positive events per volume was determined with a BD Accuri C6 Flow Cytometer.

SERT surface expression

2×10^6 platelets in diluted whole blood (modified Tyrode's buffer) were stained for 15 min with FITC-conjugated Anti-Serotonin Transporter (Alomone Labs) antibody and to APC-labeled antibody to CD41a, fixed for 10 min with 1% formaldehyde and analyzed with a BD Accuri C6 Flow Cytometer. SERT expression is expressed as median fluorescence intensity in the CD41a+ events.

Integrin $\alpha IIb\beta 3$ activation

2×10^6 platelets in diluted whole blood (modified Tyrode's buffer containing 1 mM CaCl₂) were not treated or activated with 25 μM ADP in the presence of JON/A-PE (2 μg/mL), antibody specific for the active conformation of integrin $\alpha IIb\beta 3$. Following 10 min of incubation, samples were diluted with PBS and analyzed immediately with a BD Accuri C6 Flow Cytometer.

Platelet leukocyte aggregates

50 μL of anticoagulated whole blood was incubated with APC-labeled antibody to CD41a (1:100) and PerCP-Cyanine5.5-labelled antibody to CD45 (1:200) for 15 min at room temperature. Fixation and red blood cell lysis were performed with 1 mL of BD FACS lysing solution for 10 min. Samples were acquired with a BD Accuri C6 Flow Cytometer and analyzed with FlowJo software. Platelet-leukocyte aggregates (PLA) were identified based on the expression of CD41a among CD45⁺ leukocytes.

Measurement of 5-HT by ELISA

The indicated brain regions (whole hippocampus, PFC, amygdala, hypothalamus) of mice were disrupted with a homogenizer and analyzed for serotonin content using a sandwich ELISA, following the manufacturer's instructions (5-HT ELISA kit ab133053 Abcam). Briefly, 96-well ELISA microplates were coated with specific monoclonal Ab. Samples or standard were added at the appropriate dilution and incubated for 2 h at room temperature. After careful washing, biotinylated goat anti-5-HT was added to each well; horse-radish peroxidase was used as secondary Ab and optical density was read at 450 nm.

In vivo microdialysis

Vertical concentric dialysis probes were prepared with AN69 fibers (Hospal Dasco, Bologna, Italy) as previously described in Di Chiara et al., 1993.⁶⁵ The total length of the probe was 5 mm (dialysis membrane length 3 mm, o.d. 0.24 mm). Membranes were tested for *in vitro* recovery before surgery.

Mice, anesthetized with Zoletil and Rompun, were mounted on a stereotaxic frame (David Kopf Instruments) and probes were unilaterally implanted in ventral hippocampus (AP – 3.0, ML ± 2.7 from bregma, according to Brain mice atlas (Franklin and Paxinos, 2004)) 24–36 h before experiments. On the day of the experiment each animal was placed in a circular cage. The microdialysis probe was connected to a CMA/100 pump (Carnegie Medicine) through PE-20 tubing and an ultra-low torque multichannel power-assisted swivel (Model MCS5, Instech Laboratories) to allow free movement. Artificial cerebrospinal fluid (aCSF; in mM: NaCl 140; KCl 4; CaCl₂ 1.2; MgCl₂ 1) was pumped through the dialysis probe (2.1 μL/min). Following the start of the dialysis perfusion, mice were left undisturbed for ~1 h before the collection of six baseline samples to calculate the average basal concentration. Dialysate samples were collected every 20 min for 120 min. Each dialysate sample (20 μL) was analyzed for the 5-HT concentration by UHPLC. Concentrations (pg/μL) were corrected for probe recovery. The UHPLC system consisted of an UltiMate 3000 (Thermo Fisher Scientific S.p.A.) system and a coulometric detector (UltiMate 3000 ECD-3000RS) provided with an analytical cell (6011RS ultra Coulometric Cell). The electrode 1 was set at 100 mV, and the electrode 2 at 250 mV. A C18 column (ACCLRLSLC PA2 2.2U2.1 × 100, Thermo Fisher Scientific S.p.A) maintained at 35 °C was used. The flow rate was 0.25 mL/min. A Sentry Guard precolumn (ACCLAIM, V-2 GUARD) was also used. The mobile phase consisted of methanol (7%) in Na phosphate buffer (0.1 M), Na₂EDTA (1.3 mM), and 1-octane sulfonic acid Na salt (0.25 mM), at pH = 3.65. The detection limit of the assay was 0.1 pg. Differences between basal 5-HT levels in IgG and aNK1.1 treated mice were analyzed with unpaired t test.

Immunostaining

Mice were anesthetized and intracardially perfused with PBS and then 4% formaldehyde; brains were then isolated, fixed in 4% formaldehyde and snap frozen. Cryostat sections (20 μm) were washed in PBS, blocked (3% goat serum in 0.3% Triton X-100) for 1 h, at RT, and incubated overnight at 4°C with specific antibodies diluted in PBS containing 1% goat serum and 0.1% Triton X-100. The sections were incubated with the following primary Abs: anti-c-fos 1:500; anti-5-HT 1:100; anti-Parvalbumin 1:500. For all the antibodies staining, coronal sections were first boiled for 20 min in citrate buffer (pH 6.0) at 95°C–100°C. After several washes, sections were stained with the fluorophore-conjugated antibody and Hoechst for nuclei visualization and analyzed using a fluorescence microscope. For co-immunofluorescence, the secondary antibody was subsequently used. Images were digitized using a CoolSNAP camera (Photometrics, Tucson, USA) coupled to an ECLIPSE Ti-S microscope (Nikon, Tokyo, Japan). Fos immunopositive neurons were counted manually using MetaMorph 7.6.5.0 image analysis software (Molecular Device, San Jose, USA). c-Fos+ neurons were determined only when nuclear expression of c-Fos co-localized with Hoechst 33342 staining.

Two photon microscopy analyses

Mice were anesthetized with a dose of zoletil 50 mg/kg (Virbac, France) and rompun 30 mg/kg (Bayer, Germany). The anesthesia was sufficient to immobilize the animal without overly depressing respiration or causing other complications. Each mouse was kept at 37°C using a heating plate. The scalp was resected to expose the entire dorsal surface of the skull. The periosteum was removed, but the bone was left intact. After exposing the skull, a circular craniotomy was made over the right hemisphere (3 mm

in diameter, –1.5 mm from the bregma and 2.5 mm from the midline). An optical window with a diameter of 5 mm was installed above the craniotomy using a round cover glass. To increase the anchoring strength between skull and coverglass, a layer of dental cement (Tetric Evoflow) was applied to the skull, and a thicker layer of dental cement (Sun Medical) was applied on top. Both materials were cured with UV light. Then a custom titanium headbar (Micromecc s.r.l.) were inserted over optical windows, and the gap between the headbar and the skull was sealed with dental cement.

Prior to imaging, all surgically treated mice were fully anesthetized with the anesthetic conditions used in the surgery described above. We developed an intravital chamber that minimized respiratory movement artifacts yet maintained tissue viability (Micromecc s.r.l.). For blood vessel staining mice were treated intravenous (i.v.) with tetramethylrhodamine(TRITC)-dextran 70 (5%), a high-molecular weight dextran to prevent its leakage from the vasculature (catalog n.TD70, TdB Labs, Sweden). In order to stain intravascular platelets, X488 antibody was i.v. injected in mice immediately before image acquisition. Simultaneous multicolor *in vivo* imaging was obtained by laser scanning microscopy Ultima1Pplus (Bruker). A high-resolution image stack is collected from a region within the window using a 20 \times water-immersion objective. Three-dimensional rendering of the high-resolution image stacks were collected from each mouse. Image acquisition operated under software control (Prairie View Imaging, Bruker). Post-acquisition image analysis was carried out using the FIJI software. During analysis, firstly a unique identity code was allocated for each blood vessel within a ROI. The area of the blood vessel was derived by measuring length and breadth. Pial vessels are visible on the dorsal surface. The direction of blood flow within the tributaries of the blood vessel was carefully assessed. Diverging vessels without flow of blood were classified as arteries and converging vessels with inflow of blood were classified as veins. Penetrating arterioles were identified as those vessels having relatively constant diameter. Penetrating venules, in contrast, were identified as those with more branches, and an increasing diameter moving toward the cortical surface. Based on its breadth, the blood vessel was classified as a microcapillary (6–8 μ m), a small (8–20 μ m), or large blood vessel (>20 μ m). The analysis was performed on vessels smaller than 10 μ m. For each mouse, 3–4 videos were sampled at different sites across the window, and videos were screened in a blinded fashion and excluded from analyses if stable imaging was not maintained, or if large blood vessels were in the sample region. Platelets were identified by size and green fluorescence intensity, and then platelet adhesion events were quantified by tracking platelets that did not move more than 2 μ m/s between consecutive frames, whereas non-adhesive free-flowing or transiently adhesive platelets were observed to appear and disappear between frames. Image sequences were captured at 0.91 frames/s for 5 min in x-y-t axis. x-y-t data were collected sometimes combined with 3-dimensional z stacks to create x-y-z-t time lapse images.

Hippocampal slices preparation

Animals were decapitated under halothane anesthesia. Whole brains were rapidly removed from the skull and immersed in an ice-cold artificial cerebrospinal fluid (ACSF) solution containing (in mM): 87 NaCl, 75 Sucrose, 2 KCl, 7 MgCl₂, 0.5 CaCl₂, 25 NaHCO₃, 1.2 NaH₂PO₄ and 10 glucose, pH 7.3, 300–305 mOsm. The ACSF was continuously oxygenated with 95% O₂ and 5% CO₂ to maintain the physiological pH. Transverse hippocampal slices (300 μ m thick) were cut at 4°C using a Vibratome (ThermoScientific HM 650 V) and placed in a chamber filled with ice-cold oxygenated ACSF. Brain slices were allowed to recover at least for 1 h before recording at room temperature, then transferred to a recording chamber within 1–6 h after slice preparation.

Extracellular field recordings

For field recordings, after 2 h of recovery at 30°C in an incubation chamber containing oxygenated ACSF, individual slices were transferred to the interface slice-recording chamber (BSC1, Scientific System Design Inc) where they were maintained at 30°C–32°C and constantly superfused with oxygenated ACSF at the rate of 1.5 mL/min. Solutions were applied to the slices using a peristaltic pump (Bio-Rad). Slices were visualized with a Wild M3B (Heerbrugg, Switzerland). Experiments were performed from 1 to 7 h after slicing. At the beginning of each recording, a concentric bipolar stimulating electrode (SNE-100 \times 50 mm long Elektronik-Harvard Apparatus GmbH) was placed in the hippocampus CA1 *stratum radiatum* (SR) for stimulation of the Schaffer collateral pathway projections to the CA1. A glass micropipette (0.5–1 M Ω) filled with ACSF was placed in the CA1 hippocampal region, at 200–600 μ m from the stimulating electrode, to record orthodromically-evoked field extracellular post-synaptic potentials (fEPSP). fEPSPs were recorded and filtered (low pass at 1 kHz) with an Axopatch 200A amplifier (Axon Instruments, CA) and digitized at 10 kHz with an A/D converter (Digidata 1322A, Axon Instruments). Stimuli consisted of 100 μ s constant current pulses of variable intensity, applied at 0.05 Hz. In each experiment, stimulus intensity was adjusted to evoke ~50% of the maximal fEPSP amplitude without appreciable population spike contamination. Evoked responses were monitored online and stable baseline responses (variation in the amplitude values under 10%) were recorded for at least 10 min. Only slices showing stable fEPSP amplitudes were included in the experiments. LTP was induced by high-frequency stimulation (HFS, 1 train of stimuli at 100 Hz of 1 s duration). To analyze the time course of fEPSP amplitude, the recorded fEPSP was routinely averaged over 1 min ($n = 3$ traces). fEPSP amplitude changes following the LTP induction protocol were calculated with respect to the baseline (35 min after versus 1 min before LTP induction). Data were stored on a computer using pClamp 10 software (Axon Instruments) and analyzed offline with Clampfit 10 program (Axon Instruments).

Electrophysiological data were analyzed using SigmaPlot software, statistical significances were assessed by Student's t-test, normality was verified with Shapiro-Wilk test.

Patch-clamp recordings

Whole-cell patch clamp recordings were performed on CA1 pyramidal neurons at 30°C (TC234-C Multichannel system) by using a Multiclamp 700B amplifier (Molecular Devices, USA). The ACSF (composition in mM: NaCl 125, KCl 2, CaCl₂ 1.2, NaH₂PO₄ 1.2, NaHCO₃ 25, glucose 10) was perfused at a rate of approximately 2 mL/min by using a gravity-driven perfusion system. Glass

electrodes (3–4 MΩ) were pulled with a vertical puller (PC-10, Narishige) and filled with an intracellular solution containing 145 mM Cs Methanesulfonate, 10 mM HEPES, 0.5 mM EGTA, 2 mM Mg-ATP, 0.3 mM Na₃-GTP, and 2 mM MgCl₂ (295–300 mOsm, pH 7.2). Cell capacitance was constantly monitored over the time and experiments where access resistance changed more than 20% were discarded. Spontaneous inhibitory post-synaptic currents (sIPSCs) were recorded in ACSF by holding the cell at the reversal potential of glutamatergic currents (0 mV). Signals were acquired (sampling 10 kHz, low-pass filtered 2 kHz) with DigiData-1440A using pCLAMP-v10 software (Molecular Devices, USA). Analysis of sIPSCs was performed offline on traces post hoc filtered at 1 kHz using MiniAnalysis software (Mini Analysis, Synaptosoft Fort Lee, NJ, USA) with the threshold for detection set at 5 pA. For each cell we analyzed 1 min long recording and extracted: (i) the peak amplitude; (ii) the decay time; (iii) the rise time and the inter-event interval (IEI) for each event. Since all these values were not normally distributed, we consider the median value of each cell for each of the parameters considered. The frequency rate of the synaptic events was computed as ratio between the number of detected events and the recording length in seconds.

QUANTIFICATION AND STATISTICAL ANALYSIS

Data are shown as the mean ± S.E.M. All the measurements were taken from distinct samples. Statistical significance was assessed by Student's t test, one-way ANOVA or two-way ANOVA for parametrical data, as indicated; Holm–Sidak test was used as a post-hoc test; Mann–Whitney Rank test and Kruskal–Wallis for non-parametrical data, followed by Dunn's or Tukey's post-hoc tests. For multiple comparisons, multiplicity adjusted *p*-values are indicated in the corresponding figures. Statistical analyses comprising calculation of degrees of freedom were done using Sigma Plot 11.0, GraphPad Prism 9.0, Imaris 8 and Origin 7. For each experiment, the sample size (*n*) was chosen considering the following relation: $n \geq 2\sigma(Z_{alpha}/D)^2$, where sigma is substituted by an estimate of variance (*s*²); alpha is at 0.05 (and *Zalpha* = –2) and *D* is the difference among treatments. At weaning, pups from different colonies were mixed and mice were randomly treated. The investigators performing the different analyses always received the samples from a third laboratory member, who was not involved in that specific experiment, to ensure blinding to the group allocation.